Behavior of Eccentrically Loaded Slender High-Strength Concrete Columns.

Ahmed Yousef

Structural Engineering Department., Faculty of Engineering., El-Mansoura University., Mansoura., Egypt.,
ahmyousef@mans.edu.eg

BEHAVIOR OF ECCENTRICALLY LOADED SLENDER HIGH-STRENGTH CONCRETE COLUMNS

دراسة سلوك الأعمدة الرفيعة من الخرسانة عالية المقاومة والمعرضة لأحمال غير محورية

Ahmed M. Yousef

Lecturer, Structural Engineering Department, Faculty of Engineering, Mansoura University

خلاصة:

يقدم هذا البحث نتائج تجارب معملية أجريت لدراسة سلوك الانبعاج للأعمدة الرفيعة المصنعة من الخرسانة عالية المقاومة تحت تأثير أحمال مختلفة اللامركزية . وقد تم استخدام نتائج هذه التجارب فى لإختبار مدى إمكانية تطبيق متطلبات التصميم الواردة فى الكود المصرى والكود الأوربى والكود الأمريكى فى حالة تصميم الأعمدة الرفيعة من الخرسانة عالية المقاومة والتى تصل مقاومة الضغط المميزة للخرسانة فيها إلى ٨٥ ميجاباسكال. وقد تضمن البرنامج اختبار عدد ٢٢ عمود لها نسبة نحافة مختلفة تتراوح من ١٧,٣ إلى ٦٩,٣. وقد تم دراسة تأثير عدد من المتغيرات هى قيمة اللامركزية للحمل و المسافة بين التسليح العرضى للأعمدة ونسبة التسليح الطولى للأعمدة. وقد أوضحت النتائج المعملية أن الأعمدة النحيفة من الخرسانة عالية المقاومة ينتج عنها زيادة الحمل الأقصى بالمقارنة بمثيلتها من الخرسانة ذات المقاومة العادية. وقد تبين أن الطريقة المستخدمة فى الكود الأوربى وكذلك الطريقة المستخدمة فى الكود الأمريكى لتصميم الأعمدة النحيفة هى طريقة آمنة لتصميم الأعمدة النحيفة من الخرسانة عالية المقاومة. وقد أوضحت النتائج أن حد نسبة النحافة الفاصل بين الأعمدة النحيفة والأعمدة القصيرة المطلوب من طريقة التصميم فى الكود المصرى يحتاج إلى تخفيضه عند استخدام هذه الطريقة فى تصميم الأعمدة النحيفة من الخرسانة عالية المقاومة حيث يمكن تطبيقها بأمان للأعمدة التى نسبة نحافتها تزيد عن ٤٠.

ABSTRACT

The buckling behavior of slender High-Strength Concrete (HSC) columns under axial load with different end eccentricities has been studied experimentally. The results of these tests have been used to examine the applicability of the design requirements of Normal-Strength Concrete (NSC) columns of the Eurocode 2 (EC-2), the Egyptian code (ECC-95) and ACI 318-99 building code, when applied to slender HSC columns with a characteristic compressive strength of 85 MPa. The program included tests of 22 columns with slenderness ratios λ_i ranged between 17.3 and 69.3. The main parameters examined in this study were the values of end eccentricity of the applied axial load (e/t=0.3, 0.45 and 0.90), the transverse reinforcement ratio (ρ_v) and the longitudinal reinforcement ratio (ρ_l). The results of this experimental work showed that, slender columns constructed with HSC increased the ultimate load of the tested columns in comparison with the same columns constructed with NSC. The Model Column method used by EC-2 and also the Moment Magnifier method used by ACI 318-99 building code for the design of slender columns showed to be conservative for design of HSC slender columns. The slenderness ratio limit between short and long columns required by the ECC-95 need to be modified when applied for HSC columns. Based on the results of these tests, the second order effect should be taken into account for HSC columns when $\lambda_t > 40$ ($\lambda_b > 12$).

INTRODUCTION

The advantages of High-Strength Concrete (HSC) include greater carrying capacity, reduced dead loads, longer spans and smaller member size. For this reason, the use of HSC in columns of the high-rise buildings, among other applications, is increasing [1-3]. The reduction in column size results in significant economic benefits. However, this leads also to an increase in the slenderness ratio of columns. This has made it necessary to pay more attention to the stability of reinforced HSC columns.

There have been many experimental studies on Normal-Strength Concrete (NSC) short and long tied columns [4-9]. Experiments on HSC tied columns have been conducted by a number of researchers in recent years. However, these tests have focused on HSC short columns subjected to concentric and eccentric compression axial force [10-13]. More recently, very limited test data have been reported on slender columns with end eccentricity [14,15]. Lloyd et al. [14] tested slender HSC columns with square and rectangular cross-sections. Concrete strength of the tested columns ranged from 60-90 MPa and the slenderness ratio was 32 for square columns and 56 for rectangular columns. Mendis [15] suggested a numerical method to conduct more accurate analysis of slender columns.

Although the design of reinforced concrete columns for buckling is by now a relatively well researched subject, a variety of design methods are in use and the design requirements of the Egyptian Code (ECC-95) [16], Eurocode 2 (EC-2) [17] and ACI 318-99 building code [18] differ markedly. In addition, the design equations given in theses codes for the design of slender columns contain empirical relationships derived from tests using NSC.

In this paper, an experimental investigation to study the buckling behavior of slender HSC columns subjected to end eccentricities is presented. The results of these tests were used to examine the applicability of the design requirements of NSC columns of the ECC-95, EC-2 and ACI 318-99 building code when applied to HSC slender columns.

CODES PROVISIONS FOR DESIGN OF NON-SWAY (BRACED) SLENDER COLUMNS

EC-2

According to this code, isolated columns in non-sway structures need not be checked for second order effects (including geometrical imperfections) if the slenderness ratio (λ_i) is less than or equal to the value of (λ_{crit}) given by the following equation:

$$\lambda_{crit} = 25 \left(2 - e_{o1} / e_{o2} \right) \tag{1}$$

and

$$\lambda_i = \left(\beta . H_{col} / i \right) \tag{2}$$

where e_{o1} and e_{o2} are the actual eccentricity of the applied axial loads at the ends of the column (called the first order eccentricity) and it is assumed that $| e_{o1} | \leq | e_{o2} |$, H_{col} is the unsupported height of the column from top of floor to the bottom of the floor above, i is the radius of gyration (equal to 0.3 times the overall depth of rectangular columns) and β is the effective length factor which depends on the end conditions of the column and can be determined by means of the Nomograms given in the code (for a braced frame $\beta \leq 1.0$).

The second order effect due to buckling of the column can be calculated using the Model Column Method. This method can be applied for columns with $\lambda_i < 140$ and the first order eccentricity $e \geq 0.1$. According to this method, the second order eccentricity (δ) of such a column may be calculated as follows:

$$\delta = \frac{K_1 H_e^2}{10} \ (1/r) \tag{3}$$

and

$$K_1 = (\lambda_i / 20 - 0.75) \qquad \text{for} \quad 15 \leq \lambda_i \leq 35 \tag{4.a}$$

$$K_1 = 1.0 \qquad \text{for} \quad \lambda_i > 35 \tag{4.b}$$

where H_e is the effective length of the column ($H_e = \beta H_{col}$) and the curvature $(1/r)$ can be calculated from the following equation:

$$1/r = \frac{2.K_2.\varepsilon_{yd}}{0.9\,d} \tag{5}$$

where ε_{yd} is the design yield strain of steel reinforcement ($\varepsilon_{yd} = f_{yd}/E_s$) and d is the effective depth of the cross-section in the expected direction of stability failure. The coefficient K_2 in Eq. 5 takes account of the decrease of the curvature with increasing the axial force and is defined by the following equation:

$$K_2 = (P_{ud} - P_{sd}) / (P_{ud} - P_b) \qquad \leq 1.0 \tag{6}$$

$$P_{ud} = 0.85 f_c' \ (A_c - A_s) + f_{yd} \ A_s \tag{7}$$

Where P_{ud} is the design ultimate capacity of the section subjected to axial load only, P_{sd} is the actual design axial force and P_{bal} is the axial load which, when applied to a section, maximizes its ultimate moment capacity. For symmetrical reinforced rectangular sections, P_b may be taken as ($0.4 f_c' \ A_c$), where f_c' is the design cylinder compressive strength of concrete. f_{yd} is the design yield strength of longitudinal reinforcement, A_c is the total area of the column cross-section and A_s is the total area of the longitudinal reinforcement of the column. It will be always conservative to assume that K_2 equal to 1.0.

ECC-95

According to this code, a braced rectangular column is designed as short column if $\lambda_b = H_e/b \leq 15$ or $\lambda_i = H_e/i \leq 50$. If the column slenderness ratio exceeds this limit, the column will buckle prior to reaching its limit state of material failure. The effect of buckling can be taken in design by an additional moment (M_{add}) induced by the deflection of the column's buckled shape at the section being considered.

$$M_{add} = P \cdot \delta \tag{8}$$

where P is the applied ultimate axial load and δ is the induced deflection due to buckling which can be calculated from the following expression:

$$\delta = \frac{\lambda_b^2 \cdot b}{2000} \tag{9}$$

where b is the column dimension perpendicular to the axis of bending. According to this code, for rectangular cross section λ_b should not be taken more than 30 ($\lambda_i \leq 100$).

ACI 318-99

In nonsway frames it shall be permitted to ignore slenderness effects for compression members that satisfy:

$$\lambda_i = (\frac{k \cdot H_{col}}{i}) \leq 34 - 12 (\frac{M_1}{M_2}) \tag{10}$$

where k is the effective length factor which depends on the end restrains of the column and can be determined by means of the Jackson and Moreland Alignment Charts' given in the code (for a braced frame $k \leq 1.0$). The ratio of the moments ($M1/M2$) at the two ends of the column in a braced frame will generally be taken between +0.5 and –0.5.

For design of slender columns subjected to concentric or eccentric axial load, this code recommends the Moment Magnifier method (MM method). This method can be applied for columns with $\lambda_i \leq 100$. Let the ultimate column load and the larger end moment, from a first-order elastic frame analysis, be P_u and $M_u = P_u \cdot e$. It should be noted that, the design ultimate axial load according to the ACI code is given as follows:

$$P_u = \varphi P_n \tag{11}$$

where φ is the strength reduction factor which, for tied columns, varies linearly as the nominal axial load capacity of the column cross section, P_n, varies from P_a to zero where P_a is equal to the smaller of the balanced axial load P_{bal} or ($0.143 f_c' A_c$). If P_n is greater than or equal to P_a, the factor φ should be taken equal to 0.7, while if P_n between P_a and zero, φ should be taken equal to ($0.9 - 0.2 P_n/P_a$).

The load and the moment to be used in the design of the section are P_u and ($\delta_{ns} M_u$) where δ_{ns} is the Moment Magnification Factor which is given by the following equation:

$$\delta_{ns} = \frac{C_m}{1 - (P_u / 0.75 P_c)} \geq 1.0 \tag{12}$$

in which, C_m is the equivalent moment factor and is given by the following expression:

$$C_m = 0.6 + 0.4\frac{M_1}{M_2} \geq 0.4 \tag{13}$$

and the elastic buckling load P_c is given as follows:

$$P_c = \frac{\pi^2 EI}{(k H_{col})^2} \tag{14}$$

where EI is the flexural rigidity of column section. The value of EI shall be taken equal to one of the values given by the following equations:

$$EI_1 = \frac{0.4E_c I_g}{1 + \beta_d} \tag{15}$$

$$EI_2 = \frac{0.2E_c I_g + E_s I_{se}}{1 + \beta_d} \tag{16}$$

The modulus of elasticity of concrete is given by the following equation:

$$E_{c1} = 4730\sqrt{f_c'} \tag{17}$$

in which I_g is the moment of inertia of the gross concrete section about the centroidal axis ignoring the reinforcement, E_s is the elastic modulus of steel, I_{se} is the moment of inertia of the reinforcement about the centroidal axis of the column cross-section and β_d is the concrete creep factor. In this study, the creep of concrete was neglected. It should be noted that, ACI Committee 363 [3] recommended the use of the following equation for calculating the modulus of elasticity of HSC concrete:

$$E_{c2} = 3320\sqrt{f_c'} + 6900 \qquad \text{for } 21 < f_c' < 83 \text{ MPa} \tag{18}$$

DESCRIPTION OF COLUMN TEST UNITS

Test Specimens

A total of twenty two short and long columns divided into six groups were constructed. The columns were square in cross-section (100 mm x 100 mm) and the thickness of the concrete cover measured from the bar center to the concrete surface was 20 mm as shown in Fig. 1. The first group consists of three specimens constructed with NSC used for a comparison with the other HSC specimens. As shown in Table 1, the testing program included the following main studied parameters:

1. Three different slenderness ratios ($\lambda_i = H_e/i$) were tested ($\lambda_i = 17.3$, 52 and 69.3). The corresponding effective column heights (H_{col}) were 500 mm, 1500 mm and 2000 mm, respectively. In addition, two other values of slenderness ratios ($\lambda_i = 26$ and 41.6) were tested in order to check the minimum values required by the studied codes. It should be noted that according to ECC-95, columns can be considered as slender if $\lambda_i > 50$. According

Table (1) : Details of test specimens.

Group	Column	f_{cu} (MPa)	f_c' (MPa)	H_{col} (mm)	λ_i	λ_b	Longit. bars	Transverse Rft. Ratio (ρ_v %)	e (mm)	e/t
1	CN1	26.2	21.6	500	17.3	5.0	4φ10	1.13	30	0.30
	CN2	26.2	21.6	1500	52.0	15.0	4φ10	1.13	30	0.30
	CN3	26.2	21.6	2000	69.3	20.0	4φ10	1.13	30	0.30
2	CH1	85.1	75.8	500	17.3	5.0	4φ10	1.13	30	0.30
	CH2	85.1	75.8	750	26	7.5	4φ10	1.13	30	0.30
	CH3	85.1	75.8	1200	41.6	12.0	4φ10	1.13	30	0.30
	CH4	85.1	75.8	1500	52.0	15.0	4φ10	1.13	30	0.30
	CH5	85.1	75.8	2000	69.3	20.0	4φ10	1.13	30	0.30
3	CH6	85.1	75.8	500	17.3	5.0	4φ10	0.70	30	0.30
	CH7	85.1	75.8	1500	52.0	15.0	4φ10	0.70	30	0.30
	CH8	85.1	75.8	2000	69.3	20.0	4φ10	0.70	30	0.30
4	CH9	85.1	75.8	500	17.3	5.0	4φ12	0.70	30	0.30
	CH10	85.1	75.8	1500	52.0	15.0	4φ12	0.70	30	0.30
	CH11	85.1	75.8	2000	69.3	20.0	4φ12	0.70	30	0.30
5	CH12	83.6	74.4	500	17.3	5.0	4φ10	1.13	45	0.45
	CH13	83.6	74.4	1500	52.0	15.0	4φ10	1.13	45	0.45
	CH14	83.6	74.4	2000	69.3	20.0	4φ10	1.13	45	0.45
6	CH15	83.6	74.4	500	17.3	5.0	4φ10	1.13	90	0.90
	CH16	83.6	74.4	750	26.0	7.5	4φ10	1.13	90	0.90
	CH17	83.6	74.4	1200	41.6	12.0	4φ10	1.13	90	0.90
	CH18	83.6	74.4	1500	52.0	15.0	4φ10	1.13	90	0.90
	CH19	83.6	74.4	2000	69.3	20.0	4φ10	1.13	90	0.90

to EC-2 the minimum values of λ_i are given by Eq. (1) and Eq. (2), while according to the ACI 318-99, the minimum values of λ_i are given by Eq. (10).

2. Three different conditions of end eccentricity (e) were included in the test program (e=30, e =45 mm and e = 90 mm). The corresponding e/t ratios were 0.3, 0.45 and 0.9, as given in Table (1).

3. Two different longitudinal reinforcement ratios were used (4 φ 10 with ρ_l = 3.14% and 4 φ 12 with ρ_l = 4.52%). These ratios are within the limits allowed by the codes into consideration (1.0% ≤ ρ_l ≤ 6.0 % according to ECC-95).

4. Two transverse reinforcement ratios (ρ_v=1.13% and 0.70%) were tested. These were in the form of stirrups of bar diameter (φ6) but with two different spacing between stirrups (s= 50 mm and 80 mm, respectively). It should be noted that, for earthquake resistant design, the ECC-95 requires that s should be the least of: 8 times the smaller longitudinal bar diameter (8x10mm= 80mm); 24 times the diameter of the stirrups (24x6 mm =144 mm); half the length of the shorter column dimensions (0.5x100 =50 mm) or 150 mm.

Concrete Properties

In the HSC concrete mix design, ordinary portland cement was used in conjunction with 13 mm diameter gravel. The fine aggregate was natural sand with a fineness modulus of 2.80. The mix proportions by weight per 1.0 m^3 was: Cement 475 kg, Gravel 1180 kg, Sand 580 kg and water 120 kg. Light gray locally produced silica fume with a specific gravity of 2.15 was used with 15 percent by weight of cement. A superplasticizer with 3 percent by weight of cement was added and enough mixing time was allowed to produce uniform mix of concrete without any segregation.

Standard specimens were prepared during casting of columns to obtain the mechanical properties of the used concrete. The concrete compressive strength f_{cu} of the mix after 28 days based on an average of three cube specimens (150x150x150 mm) was 85 MPa. Additionally, the splitting cylinder tensile strength was equal to 4.82 MPa and the flexural strength (based on beams 100x100x500 mm) was equal to 8.91 MPa. Two cylinder (150 x 300 mm) were tested in uniaxial compression to determine the cylinderical compressive strength. The HSC tested specimens were constructed in 2 series included, in general, the columns tested with the same eccentricity. The cube compressive strength of the specimens f_{cu} and the cylinder compressive strength f_c' after 28 days of casting are given in Table 1.

The NSC mix proportions by weight per 1.0 m^3 was: Cement 350 kg, Gravel 1215 kg, Sand 654 kg and water 147 kg. The design concrete compressive strength f_{cu} of the mix after 28 days was 25 MPa. Additionally, the splitting cylinder tensile strength was equal to 2.02 MPa and the flexural strength was equal to 3.11 MPa.

Reinforcement

The main longitudinal reinforcement of each of the tested columns consists of four deformed high-grade bars with diameter 10 mm or 12 mm and the yield strength of these bars f_y were equal to 397.0 and 382.0 MPa, respectively, while the maximum strength were 581.0 and 602.0 MPa, respectively. The recorded strain at the initiation of yield of these bars were 1890 and 1820 $\mu\varepsilon$, respectively. The transverse reinforcement comprised 6 mm diameter mild steel bars with yield strength equal to 262.0 MPa and maximum strength equal to 376.0 MPa.

Test Setup and Instrumentation

The columns were cast in forms made of wood with smooth hard varnish surfaces. The forms were removed after 48 hours from casting and columns were moistured continuously with water for 26 days. Then, the specimens were painted white, from one face only, to facilitate crack observation and tested after 28 days of casting.

The tests were conducted in the loading frame and the test setup is shown in Fig. 2. The boundary conditions at the ends were both hinged and the end eccentricities were of the same sign as shown in Fig. 1. The lateral deflections at the midheight of the column were monitored by two dial gauges 0.01 mm accuracy. Electrical strain gauges of 120 ohm resistance and 10 mm and 5 mm length were bonded to the longitudinal reinforcement and the transverse reinforcement within the central 100 mm of the specimens. The concrete strains in the midheight of the test units were measured using mechanical strain gauge over the central 200 mm gauge length. The load was applied at increments of 0.5 or 1.0 ton up to failure and after each load increment the cracks are traced and marked according to their priority of occurrence.
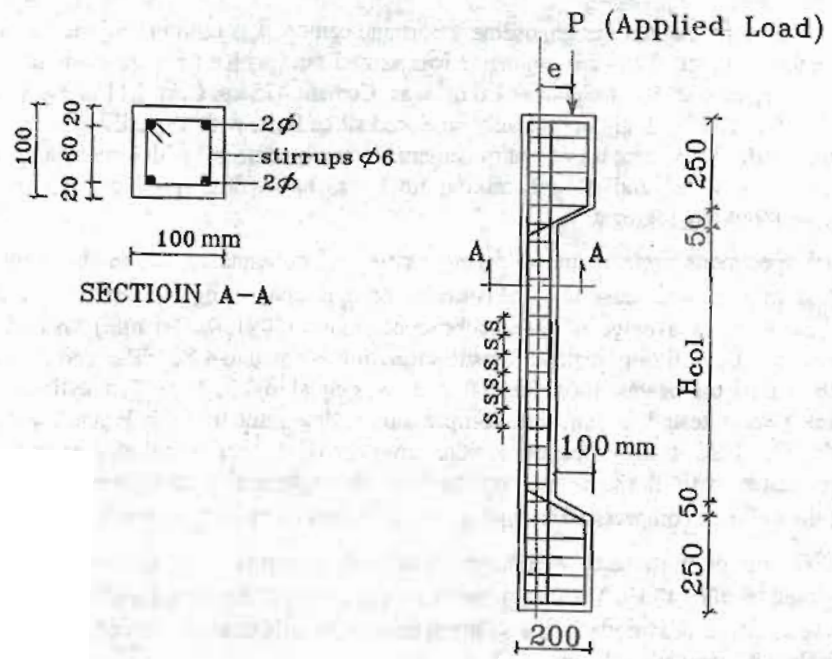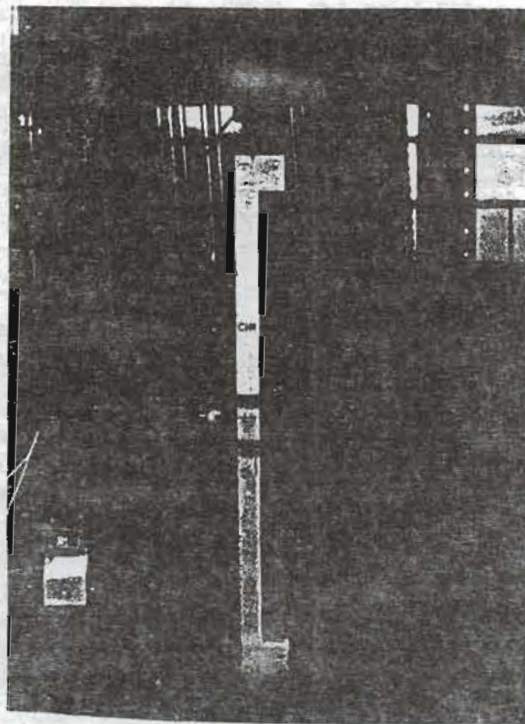
Fig. (1): Details of Column Specimens.

Fig. (2): Test setup.

RESULTS AND DISCUSSIONS

General Behavior and Ultimate Loads

The recorded ultimate loads $P_{ue,exp}$ and the corresponding lateral deflections at midheight of the tested columns δ_{exp} are given in Table 2. Specimens CH7 and CH12 failed at relatively small ultimate loads. Failure of these two specimens occurred at their ends by compression of the heads because of the imperfect compaction of the ends during casting. Therefore, these specimens were not considered in the investigation. From Table 2, upon comparing the experimental ultimate loads for the HSC and NSC columns, column CH1 (with e=30 mm, $\lambda_i = 17.3$ and $\rho_l = 3.14$ %) had an increase by 118 % over the column CN1 which has the same properties, but column CH5 ($\lambda_i = 69.3$) had an increase by only 14.0 %. This showed that the increase of the experimental ultimate load due to increasing the concrete strength is decreased with the increase in the slenderness ratio.

Generally, most of the tested columns failed at or near to the midheight. The failure mode of the columns depends mainly on the eccentricity of the applied axial load. The tested HSC columns with big eccentricity (group 5 with e=45 mm and group 6 with e=90 mm) failed by yielding of the longitudinal bars in the tension side, followed by a shift of the neutral axis toward the compression side until crushing of the concrete in the compression side of the section. It should be noted that, for group 5 and 6, the calculated balanced eccentricity (e_{bal}) using the ACI stress block was equal to 42.2 mm. For specimens tested with small eccentricity (e=30 mm), most of columns with $\lambda_i = 17.3$ and 26.0 failed at the midheight by increasing the compression strain until crushing of the concrete in the compression zone before yielding of the steel. The concrete cover, first, spalled off in the compression side and at later stages, the spalling of the cover extended to the side faces of the column. Slender specimens tested with small eccentricity (e=30mm, $\lambda_i = 52$ and 69.3) failed due to increasing the tensile steel strain at the midheight up to yielding of the longitudinal reinforcement before the compression strain reaching the crushing value. The failure mode for the NSC specimens (group 1) was approximately the same as that of the specimens of the HSC specimens (group 2). Photographs of the failure mode of some of the tested HSC specimens are shown in Fig. 3.

The type of failure of the tested specimens can be explained also from the readings of strain recorded in the longitudinal reinforcement during the tests as shown in Fig. 4. It can be seen from Fig. 4a that, for specimen CH1, the recorded compressive strain increased gradually with increasing the applied load up to crushing of the concrete in the compression zone at strain reading of about 4000 $\mu\varepsilon$, while the tensile steel strains was far from yielding. For specimens CH4 and CH5 with $\lambda_i = 52$ and 69.3, respectively, the compressive strains increased gradually but the tensile strains increased with a higher rate than that of the short columns CH1. In this case, because of the additional moment due to buckling of columns, the yielding of the longitudinal reinforcement in the tension side reached at low levels of compressive strains. For specimens with big eccentricity (group 6 with e=90 mm), it can be seen from Fig. 4b that, yielding of the longitudinal reinforcement occurred always sooner at low values of compressive strains in the compression zone. For example, the compressive strain in specimen CH17 was equal to (-805$\mu\varepsilon$) at yielding of steel in the tension side at +1890$\mu\varepsilon$.
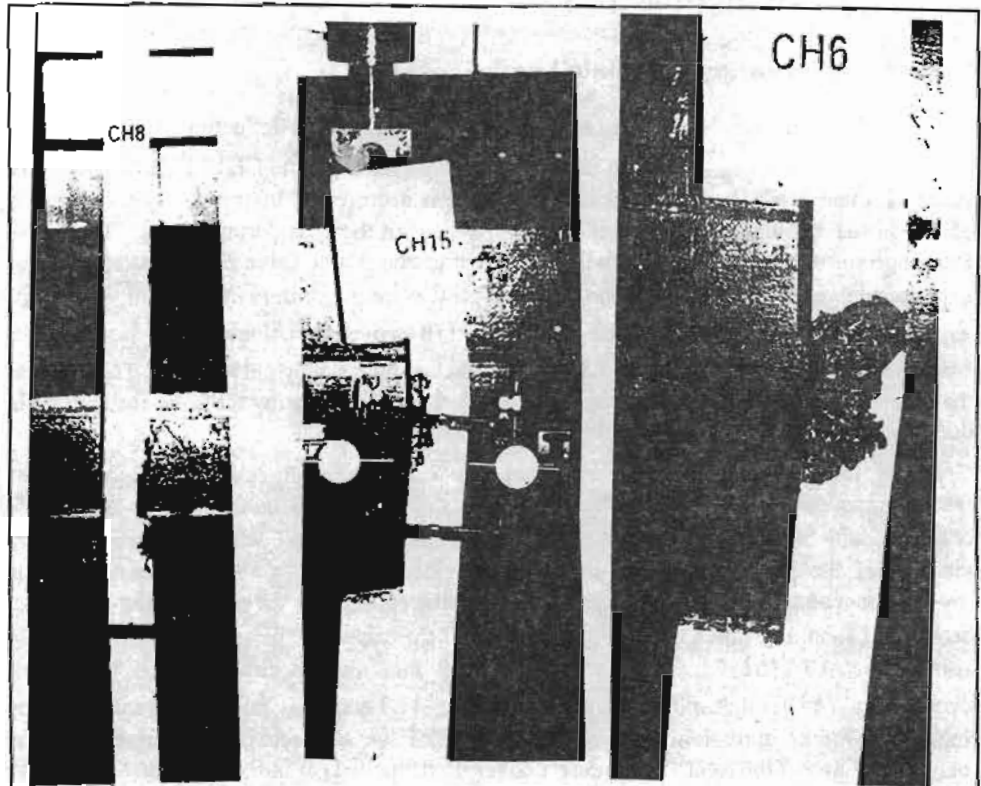
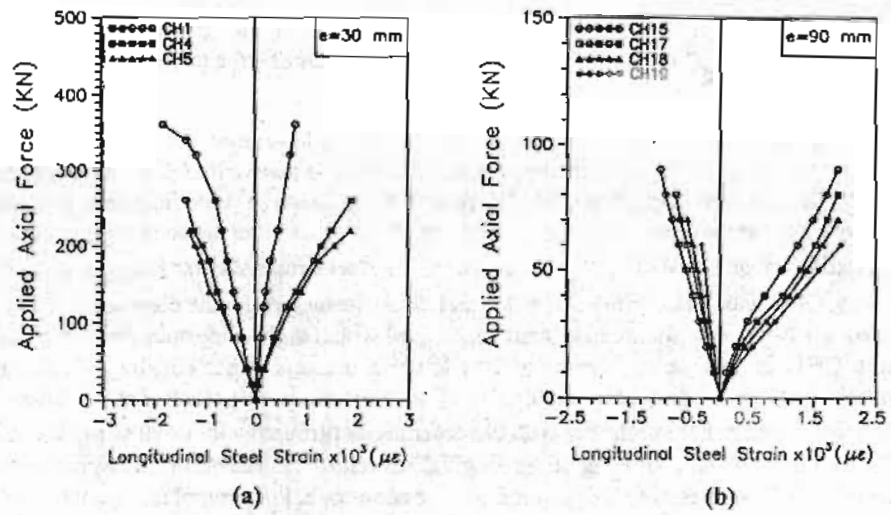Fig. (3): Photographs of the failure mode of some of the tested columns.

(a)   (b)

Fig. (4): Strains in the longitudinal bars of some of the tested columns.

Effect of Longitudinal Reinforcement Ratio

The results of the tests of specimens with the same properties but with different longitudinal reinforcement ratios ρ_l showed that the recorded ultimate load was dependent also on the value of ρ_l. Figure 5 illustrates the effect of the longitudinal steel ratio on the ultimate load of the column. The calculated values of P_n and the ratio (P_{uexp}/P_n) for the tested specimens are reported in Table 2, where P_n is the nominal capacity of the column section for the case of $\lambda_i = 0$ with the given eccentricity (e=30 or 45 or 90 mm). It should be noted that, the stress block of ACI 318-99 code (taking $\varepsilon_{cu} = 0.003$) was used in calculation of the values of P_n. The ratio (P_{uexp}/P_n) for group 2 (ρ_l=3.14 %) and group 4 (ρ_l=4.52 %) show a small difference when the columns are relatively long, but the difference is increased with the decrease in slenderness ratio. Therefore, in this case, an increase of longitudinal steel ratio leads to a larger increment of (P_{uexp}/P_n) value for a short HSC column than for a slender column.
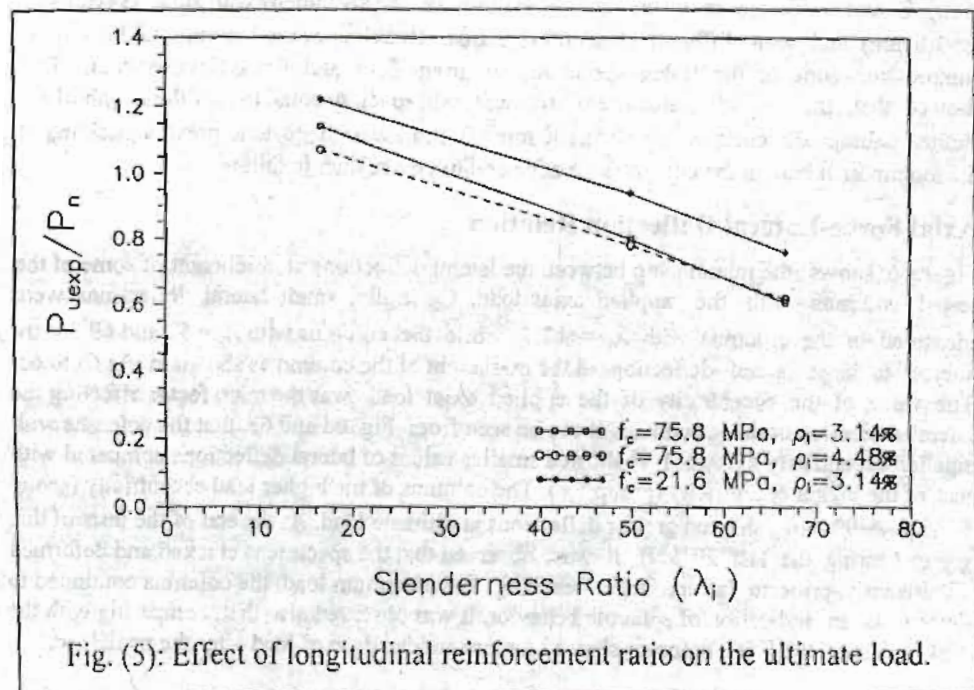
Effect of Transverse Reinforcement

The test program included two transverse reinforcement ratios, which were in the form of the same stirrup bar diameter (ϕ 6) but with two different stirrups spacing (s = 50 mm and 80 mm). The results of the columns of group 3 (s = 80 mm) and the similar columns of group 3 (s = 50 mm) showed that the recorded ultimate load of specimens of group 3 were less than that of group 2 but with little differences. Specimens CH6 and CH7 of group 3 failed in a sudden explosive manner. At the time of failure, the cover concrete spalled and the longitudinal bars in the compression zone buckled. This type of failure occurred also for the specimens of group 4 (s=80 mm and ρ_l = 4.52 %). The provided transverse reinforcement of group 2 was sufficient to insure ductile failure for the specimens with small eccentricity (e=30 mm) and with different slenderness ratios. Buckling of the longitudinal bars in the compression zone of the tested specimens of group 3, 5 and 6 was not observed. This showed that, the provided lateral reinforcement with spacing equal to half the length of the shorter column dimensions (s = 0.5x100 mm=50 mm) was adequate to prevent buckling of the longitudinal bars in the compression zone and to ensure ductile failure.

Axial Force-Lateral Deflection Relation

Figure 6 shows the relationship between the lateral deflections at midheight of some of the tested columns with the applied axial load. Generally, small lateral deflections were measured in the columns with λ_i = 17.3, while the columns with λ_i = 52 and 69.3 were subject to large lateral deflections at the midheight of the column as shown in Fig.6a to 6c. The value of the eccentricity of the applied axial load was the main factor affecting the lateral deflection of the specimens. It can be seen from Fig. 6d and 6e, that the columns with smaller eccentricity (group 1-4) showed smaller values of lateral deflections compared with that of the bigger eccentricity (group 5,6). The columns of the higher load eccentricity (group 6 with e=90 mm) showed greater deflections at ultimate load. At the end of the tests of this group (during the last 20 kN), it was observed that the specimens cracked and deformed significantly prior to failure. After reaching the maximum load, the columns continued to deform as an indication of a ductile behavior. It was observed also that, comparing with the NSC columns, the HSC columns showed a more sudden drop of load after the peak load.

Table (2) : Summary of test results

Group	Column	λ_i	P_{uexp} (kN)	P_n (kN)	δ_{uexp} (mm)	(P_{uexp}/P_n)
	CN1	16.7	188.5	154.3	4.55	1.22
1	CN2	50.0	145.7	154.3	9.60	0.94
	CN3	66.7	117.1	154.3	13.20	0.76
	CH1	16.7	411.4	359.8	5.05	1.14
	CH2	25.0	368.6	359.8	5.90	1.02
2	CH3	40.0	305.7	359.8	7.30	0.85
	CH4	50.0	288.6	359.8	9.40	0.80
	CH5	66.7	220.0	359.8	12.40	0.61
3	CH6	16.7	400.0	359.8	5.30	1.11
	CH8	66.7	211.4	359.8	11.90	0.59
	CH9	16.7	420.0	391.5	5.20	1.07
4	CH10	50.0	305.7	391.5	10.20	0.78
	CH11	66.7	242.9	391.5	13.10	0.62
5	CH13	50.0	200.0	251.7	12.20	0.79
	CH14	66.7	157.1	251.7	15.90	0.62
	CH15	16.7	102.9	80.6	5.90	1.28
	CH16	25.0	97.1	80.6	7.10	1.20
6	CH17	40.0	88.6	80.6	9.80	1.10
	CH18	50.0	80.0	80.6	13.40	0.99
	CH19	66.7	71.4	80.6	18.60	0.89

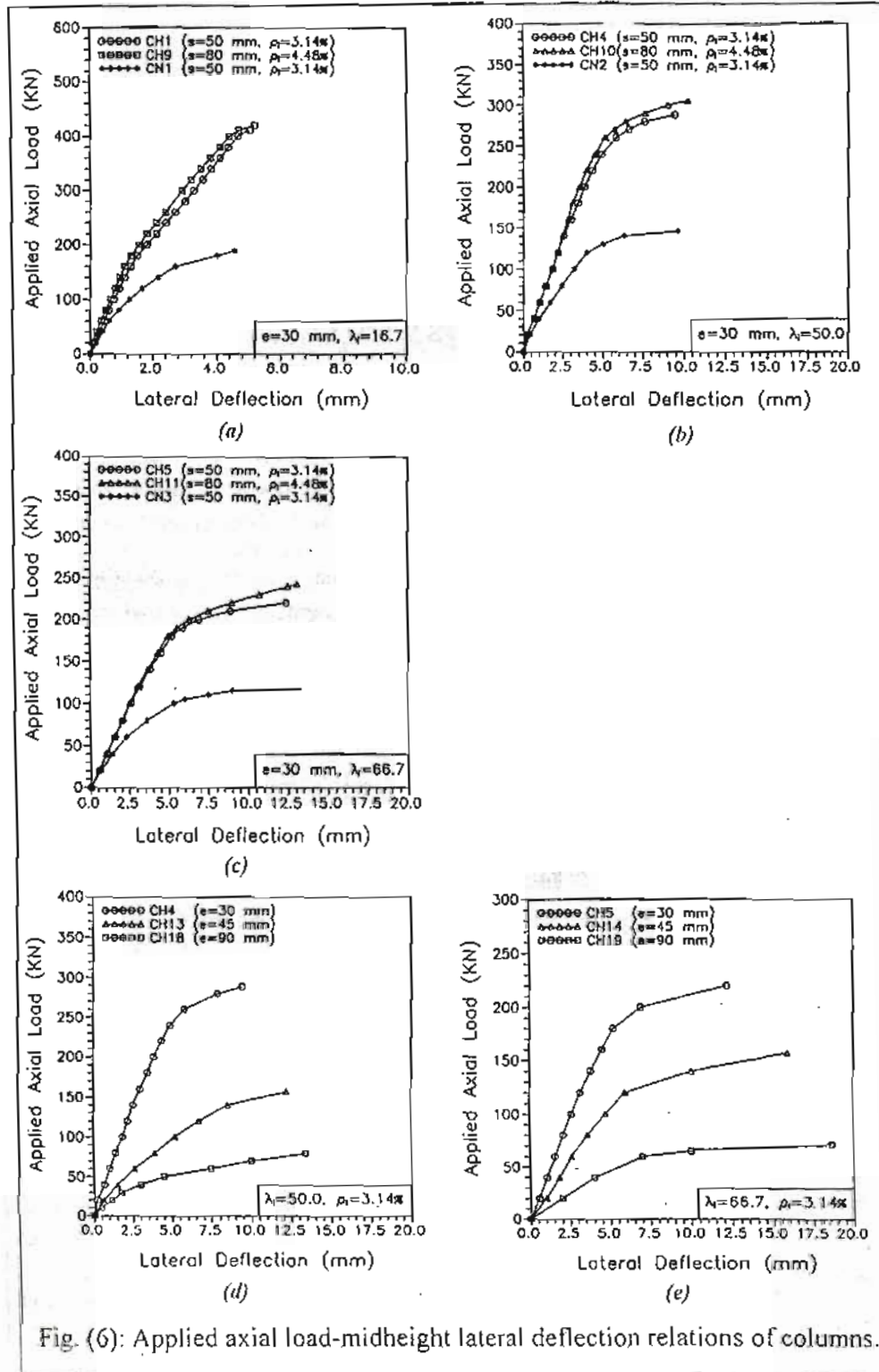Fig. (5): Effect of longitudinal reinforcement ratio on the ultimate load.

Fig. (6): Applied axial load-midheight lateral deflection relations of columns.

The applied load-lateral deflection relationships for the specimens of group 3 (ρ_v=0.7%) were approximately the same as that of the similar specimens of group 2 (ρ_v=1.13%). This indicates that the transverse reinforcement ratio (ρ_v) has negligible effect on the lateral deflection of the tested specimens. As shown in Table (2), the lateral deflections at ultimate loads (δ_{uexp}) for the columns of λ_i = 17.3 show a little increase with the increase in concrete strength, however, for the columns of λ_i = 69.3 they decreased. Increasing the longitudinal reinforcement ratio of the tested HSC columns with the same applied eccentricity (group 3 and group 5) increased by a very small percent the lateral deflections at ultimate loads for all the tested slenderness ratios as shown from Fig. 6a to 6c.

COMPARISON OF TEST RESULTS WITH CODES REQUIREMENTS

The design methods for reinforced concrete slender columns of the ECC-95 and EC-2 were used to predict the ultimate load of the HSC and NSC columns of this study. The predicted values of ultimate lateral deflection at the midheight of the tested columns due to the second order effect (δ_{ud}) using the equations of ECC-95 and EC-2 are given in Table (3). In calculating δ_{ud} according to EC-2, the coefficient K_2 in Eq. 5 was taken equal to 1.0. It can be seen that, although the two codes use different methods for predicting the ultimate lateral deflection of the slender columns, the predicted values for the tested specimens with different applied eccentricity were approximately similar for columns with λ_i greater than 40. The recorded experimental ultimate lateral deflection (δ_{uexp}) showed to be, generally, less than that predicted by the two codes for higher slenderness ratios while it was more than that predicted for lower slenderness ratio.

A comparison between the recorded experimental ultimate axial load (P_{uexp}) with the predicted values (P_{ud}) using those two codes are given also in Table (3). The values of P_{ud} was calculated from the equilibrium between the external forces (with the applied eccentricity e= 30 or 45 or 90 mm in addition to δ_{ud} as calculated for each code) and the internal forces of the section. The capacity reduction factor φ was adopted as unity in calculating P_{ud} according to the two codes. It should be noted that, a rectangular stress block of maximum stress equal to ($0.85 f_c^{'}$) and the ultimate concrete strain equal to 0.003 was used in calculation of the values of P_{ud} for the two codes. The ECC-95 predictions were generally conservative for thirteen columns from a total of seventeen HSC columns with a mean (1.079) despite that the ECC-95 design equation is empirical and neglects the effect of many factors. The predictions of the model column method adopted in EC-2 were also conservative for fifteen columns from the tested seventeen HSC columns with a mean slightly more than that of the ECC-95 (1.112). For the two codes, the conservatism slightly decreased with increasing the slenderness ratio and considerably increased with increasing the applied eccentricity. For NSC columns the conservatism was more than that of the similar HSC columns. The tested slender columns of group 3 (λ_i =52, ρ_v= 0.70 % and ρ_l=3.14%) as well as that of group 4 (λ_i=52 and 69.3, ρ_v= 0.70 % and ρ_l = 4.52 %) showed to be slightly unconservative for the two codes. This seems to be due to the reduction in ρ_v from 1.13% to 0.70% (increase in stirrup spacing from 50 mm as required by the ECC-95 to 80 mm) which resulted in a sudden brittle failure at relatively smaller ultimate load.

It should be noted that, for the tested columns in Table (3), the EC-2 neglects the second order effects for the columns with $\lambda_i \leq 25$. It is of great interest that ECC-95 considered the columns with $\lambda_i < 50$ as short columns and the columns with $\lambda_i > 50$ as long columns. For the ECC-95, the predicted ultimate force of the tested column CH3 with small eccentricity ($e=30$ mm and $\lambda_i =41.6$) was unsafe because of neglecting the second order effect, while according to the EC-2 the predicted ultimate force for the same column was conservative. This means that, in order to apply the present method of ECC-95 for design of slender HSC columns, the limits of the slenderness ratio for short columns need to be reduced. Based on the results of this experimental work, the ECC-95 method can be safely and conservatively applied to HSC columns with λ_i more than λ_{cri} as given in EC-2 by Eq. 1, but for simplicity, λ_{cri} can be taken equal to 40.

In order to compare the recorded experimental ultimate axial load with the predicted values using the Moment Magnifier method used by ACI 318-99 code, Figure 7 was used. This figure shows the ratio of (P_u /P_n) calculated by the MM method with these obtained from the tests of some specimens. Four values of ultimate loads were calculated using Equations 15 to 18. These values were referred to as $P_{udACI11}$, $P_{udACI12}$, $P_{udACI21}$ and $P_{udACI22}$. These correspond to the calculated ultimate load using the modulus of elasticity E_{C1} (Eq. 17) and E_{C2} (Eq. 18), respectively. Each value of E_C resulted in two values of the flexural rigidity (EI_1 calculated using Eq. 15 and EI_2 calculated using Eq. 16). For example, $ACI12$ means the values calculated using E_{C1} and EI_2. It should be noted that, in calculating the flexural rigidity EI, the creep of concrete in the form of the concrete creep factor β_d was ignored.

It can be seen from Fig. 7a, that (P_u /P_n) values for the HSC columns ($e=30$ mm) are smaller than those for the NSC columns for all the tested slenderness ratio. The (P_u /P_n) values for the HSC and NSC columns show a small difference in the case of $\lambda_i = 17.3$, and a larger difference with increasing λ_i. A relatively small (P_u /P_n) values for the tested slender HSC columns were recorded. This was due to the second-order effect, i.e., the ultimate load is reduced by the amplified bending moment caused by lateral deflection. For the HSC specimens tested under small eccentricity, the four methods of the ACI code were conservative. It should be noted that in calculating the moment magnification factor δ_{ns}, the design ultimate axial load was calculated as given by Eq. 11. For the tested HSC columns with small eccentricity, the calculated values of P_u exceeded the value of ($0.75 P_c$) for the columns $\lambda_i = 69.3$, and as a result, δ_{ns} was negative. This means that the stiffness is lower than expected and the ACI 318-99 code requires that the column cross-section to be enlarged. For the same reason, the calculated values of δ_{ns} were more than 2.0 for some columns with $\lambda_i < 69.3$.

For the tested columns of big eccentricity (group 6), Fig. 7b showed that the ratio (P_u/P_n) for all the specimens of this group were more than that predicted by the ACI methods. The level of conservation decreased with increasing the slenderness ratio. It should be noted that the calculated values of δ_{ns} for this group were more logical than that of group 3. It can be seen from Fig. 7a and b, that the predicted axial ultimate load of the tested HSC columns using the equation of E_c proposed by ACI Committee 363 (Eq. 18) was more conservative than that predicted using Eq. 17 used by the ACI 318-99.

Table (3): Comparison of test results with the ECC-95 and EC-2 Predictions.

Group	Column	δ_{uexp} (mm)	P_{uexp} (kN)	ECC-95		$\dfrac{P_{u\,exp}}{P_{dECC-95}}$	EC-2		$\dfrac{P_{u\,exp}}{P_{dEC-2}}$
				δ_{ud} (mm)	P_{ud} (kN)		δ_{ud} (mm)	P_{ud} (kN)	
1	CN1	4.55	188.5	1.25	154.3	1.222	0.112	154.3	1.222
	CN2	9.60	145.7	11.25	125.6	1.160	11.81	123.1	1.184
	CN3	13.2	117.1	20.00	108.2	1.082	21.00	106.7	1.097
2	CH1	5.05	411.4	1.25	359.8	1.143	0.112	359.8	1.143
	CH2	5.90	368.6	2.81	359.8	1.024	1.48	348.7	1.057
	CH3	7.30	305.7	7.20	359.8	0.850	7.56	302.0	1.012
	CH4	9.40	288.6	11.25	278.5	1.035	11.81	275.5	1.047
	CH5	12.40	220.0	20.00	219.5	1.002	21.00	213.3	1.031
3	CH6	5.30	400.0	1.25	359.8	1.096	0.112	359.8	1.096
	CH8	11.9	211.4	11.25	219.5	0.963	11.81	213.3	0.991
4	CH9	5.20	420.0	1.25	391.5	1.073	0.107	391.5	1.073
	CH10	10.20	305.7	11.25	307.0	0.995	11.37	305.8	1.000
	CH11	13.10	242.9	20.00	258.4	0.940	20.22	256.8	0.946
5	CH13	12.20	200.0	11.25	181.5	1.102	11.81	178.6	1.120
	CH14	15.90	157.1	20.00	142.3	1.104	21.00	137.2	1.145
6	CH15	5.90	102.9	1.25	80.6	1.277	0.112	80.6	1.277
	CH16	7.10	97.1	2.80	80.6	1.205	1.48	78.4	1.239
	CH17	9.80	88.6	7.20	80.6	1.099	7.56	70.4	1.258
	CH18	13.40	80.0	11.25	66.4	1.205	11.81	65.5	1.219
	CH19	18.60	71.4	20.00	58.0	1.231	21.00	57.1	1.250

Fig. (7): Comparison of test results with the ACI 318-99 predictions.
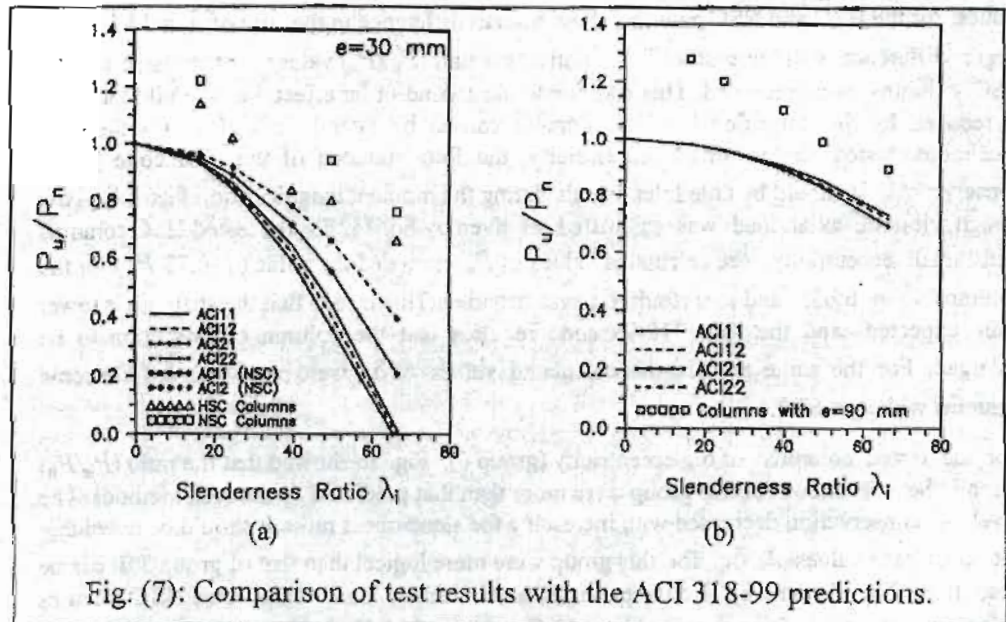
CONCLUSIONS

Based on the results of this experimental investigation on the behavior of eccentrically loaded slender HSC columns with concrete cube compressive strength of about 85.0 MPa, the following can be concluded:

1. Slender columns constructed with HSC had increased ultimate load in comparison with the same columns constructed with NSC. Increasing the longitudinal reinforcement ratio slightly increased the ultimate load, while increasing the applied eccentricity increased the midheight lateral deflection and decreased the ultimate load.

2. The failure mode of the columns depends mainly on the magnitude of the eccentricity of the applied axial load. HSC columns tested with big eccentricity failed by typical flexural manner. HSC columns with small eccentricity (e/t =0.3) and slenderness ratio $\lambda_i < 25$ failed by crushing of the concrete before yielding of the tensile reinforcement, while the columns with $\lambda_i > 25$ failed due to increasing the tensile steel strain at the midheight up to yielding of the longitudinal reinforcement before the compression strain reached the crushing value.

3. The transverse reinforcement required by the ECC-95 for NSC columns was sufficient to ensure ductile failure of the tested short and slender HSC columns subjected to small and big end eccentricity.

4. The Model Column method used by EC-2 for design of slender columns showed to be slightly conservative for design of HSC slender columns. The Moment Magnifier method used by ACI 318-99 building code was safe and conservative.

5. Although the ECC-95 equation for predicting the second order effect of slender columns is empirical and neglects the effect of many factors, the results showed that this equation was conservative for the design of slender columns.

6. The slenderness ratio limit between the short and long columns required by the ECC-95 need to be reduced when applied for HSC columns. Based on the results of these tests, the second order effect should be taken into account for HSC columns with $\lambda_i > \lambda_{cri}$ used by the EC-2 and given by Eq. (1), but for simplicity, λ_{cri} can be taken more than 40 ($\lambda_b > 12$).

ACKNOWLEDGEMENT

REFERENCES

1. ACI-ASCE Committee 441 (1997), " High-Strength Concrete Columns: State of the Art," ACI Structural Journal, V. 94, No. 3, May-June 1997, pp. 323-335.

2. Collins, M. P., Mitchell, D., and MacGregor, J. G. (1993), "Structural Design Considerations for High-Strength Concrete," Concrete International, V. 15, No. 5, May 1993, pp. 27-34.

3. ACI Committee 363 (1992), " State-of-the-Art Report on High-Strength Concrete ", ACI 363R-92, American Concrete Institute, Detroit, 1992, 55 p.

4. Sheikh, S. A., and Uzumeri, S. M. (1980), "Strength and Ductility of Tied Concrete Columns," Journal of the Structural Division, ASCE, V. 106, No. ST5, May 1980, pp. 1079-1102.

5. El-Gohary, H. (2001), " Strength and Deformations of Short Concrete Columns Under Eccentric Compression," Proceedings of the Ninth International Colloquium On Structural and Geotechnical Engineering, 10-12 April 2001, Faculty of Engineering, Ain Shams University, Paper No. RC17, Cairo, Egypt.

6. Ahmed, S. A., and El-Tuhami, A. A. (2000), " Effect of Steel Arrangement on the Behavior of RC Columns," Proceedings of the 8th Arab Structural Engineering Conference, Structural Engineering Department, Faculty of Engineering, Cairo University, 21-23 October 2000, Cairo, Egypt, pp. 805-815.

7. Goyal, B. B. and Jackson, N. (1971), "Slender Concrete Columns Under Sustained Loads," Journal of the Structural Division, ASCE, V. 97, No. ST11, November 1971, pp. 2729-2750.

8. Johnston, B. G. (1983), "Column Buckling Theory: Historic Highlights," Journal of the Structural Engineering, ASCE, V. 109, No. 9, September 1983, pp. 2086-2096.

9. Rangan, V. B. (1990), " Strength of Reinforced Concrete Slender Columns," ACI Structural Journal, V. 87, No. 1, January-February 1990, pp. 32-38.

10. Foster, S. J., Liu, J. and Sheik, S. H. (1998), "Cover Spalling in HSC Columns Loaded in Concentric Compression," Journal of the Structural Engineering, V. 124, No. 12, December 1998, pp. 1431-1437.

11. Razvi, S. R. and Saatcioglu, M. (1999), " Circular High-Strength Concrete Columns under Concentric Compression," ACI Structural Journal, V. 96, No. 5, September-October 1999, pp. 817-825.

12. Ibrahim, H. H., and MacGregor, J. G. (1996), " Tests of Eccentrically loaded High-Strength Concrete Columns," ACI Structural Journal, V. 93, No. 5, September -October 1996, pp. 585-594.

13. Abo Eleineen, A., Abd El-Faiad A. S., Zaher, A. H., and Montaser, W. M. (2000), "Behavior of High Performance Concrete Columns Under Eccentric Loading," Proceedings of the Second International Conference on Civil Engineering, Civil Engineering Department, Faculty of Engineering, Helwan University, Cairo, Egypt, 1-3 April 2000, pp. 805-815.

14. Lloyed, N. A., and Rangan, B. V. (1996), " Studies on High-Strength Concrete Columns Under Eccentric Compression," ACI Structural Journal, V. 93, No. 6, November-December 1996, pp. 631-638.

15. Mendis, P. A. (2000), " Behavior of Slender High-Strength concrete columns," ACI Structural Journal, V. 97, No. 6, November-December 2000, pp. 895-901.

16. Ministry of Building and Infrastructures (1995), " Egyptian Code for Design and Construction of Reinforced Concrete Structures," Fourth Edition, Cairo, Egypt, 1998.

17. Commission of the European Communities (1990), " Eurocode No. 2: Design of Concrete Structures ", Part 1: General Rules and Rules for Buildings, October, 1990.

18. ACI Committee 318 (1999), " Building Code Requirements for Reinforced Concrete and Commentary (ACI 318-95)," American Concrete Institute, Detroit, 1995.